



**HAL**  
open science

## Application of NO<sub>x</sub> Adsorber to Diesel Depollution: Performances and Durability

J. B. Dementhon, T. Colliou, B. Martin, M. Bouchez, M. Guyon, I.  
Messaoudi, R. Noirot, S. Michon, C. Gérentet, L. Pierron

► **To cite this version:**

J. B. Dementhon, T. Colliou, B. Martin, M. Bouchez, M. Guyon, et al.. Application of NO<sub>x</sub> Adsorber to Diesel Depollution: Performances and Durability. Oil & Gas Science and Technology - Revue d'IFP Energies nouvelles, 2003, 58 (1), pp.129-149. 10.2516/ogst:2003009 . hal-02043832

**HAL Id: hal-02043832**

**<https://ifp.hal.science/hal-02043832>**

Submitted on 21 Feb 2019

**HAL** is a multi-disciplinary open access archive for the deposit and dissemination of scientific research documents, whether they are published or not. The documents may come from teaching and research institutions in France or abroad, or from public or private research centers.

L'archive ouverte pluridisciplinaire **HAL**, est destinée au dépôt et à la diffusion de documents scientifiques de niveau recherche, publiés ou non, émanant des établissements d'enseignement et de recherche français ou étrangers, des laboratoires publics ou privés.

# Application of NO<sub>x</sub> Adsorber to Diesel Depollution: Performances and Durability

J.B. Dementhon<sup>1</sup>, T. Colliou<sup>1</sup>, B. Martin<sup>1</sup>, M. Bouchez<sup>2</sup>, M. Guyon<sup>3</sup>,  
I. Messaoudi<sup>2</sup>, R. Noirot<sup>4</sup>, S. Michon<sup>5</sup>, C. Gérentet<sup>5</sup> and L. Pierron<sup>5</sup>

<sup>1</sup> Institut français du pétrole, 1 et 4, avenue de Bois-Préau, 92852 Rueil-Malmaison Cedex - France

<sup>2</sup> Ségime, 104, avenue Kennedy, 75016 Paris - France

<sup>3</sup> Renault, 1, allée Cornuel - 91510 Lardy - France

<sup>4</sup> PSA Peugeot Citroën, 18, rue des Fauvelles, 92256 La Garenne-Colombes - France

<sup>5</sup> Renault VI, DER 1 - BP 310, 68802 Saint-Priest Cedex - France

*j-baptiste.dementhon@ifp.fr - thierry.colliou@ifp.fr - brigitte.martin@ifp.fr - matthias.bouchez@renault.com  
marc.guyon@renault.com - isabelle.messaoudi-renexter@renault.com - remi.noirot@mpsa.com  
sylvain.michon@renaultvi.com - claire.gerentet-de-saluneaux@renaultvi.com - lois.pierron@renaultvi.com*

## **Résumé — Application des pièges à NO<sub>x</sub> à la dépollution Diesel : performances et durabilité —**

Dans le but d'assurer une optimisation globale des performances d'un moteur Diesel (NO<sub>x</sub>, particules, consommation), le recours à un système de post-traitement de NO<sub>x</sub> s'avère nécessaire pour satisfaire aux normes Euro IV et suivantes. Parmi les procédés connus, le piège à NO<sub>x</sub> peut offrir des niveaux d'efficacité comparables à la réduction par l'urée sans toutefois présenter les mêmes contraintes.

Le piège fonctionne sur la base d'une alternance entre des phases de fonctionnement pauvres durant lesquelles les NO<sub>x</sub> sont stockés, et des phases riches durant lesquelles les nitrates sont déstockés et les NO<sub>x</sub> traités. Aspect important de la technologie, les pièges à NO<sub>x</sub> sont extrêmement sensibles à l'empoisonnement par le soufre, et les niveaux futurs de soufre dans les carburants envisagés rendent probable la nécessité de recourir à des stratégies de désulfatation.

Le présent article présente des résultats obtenus sur moteur VP (véhicule particulier) d'une part, et PL (poids lourd) d'autre part.

Dans le cas du véhicule particulier, l'objectif du travail consistait à étudier les effets de carburants à faible taux de soufre sur les performances du piège à NO<sub>x</sub> en application Diesel. Dans cette étude, l'influence de la géométrie des cellules du support de piège est également étudiée.

L'utilisation d'un carburant contenant 10 ppm de soufre suffit à maintenir les performances du piège à NO<sub>x</sub> lors d'un test simulant un roulage de 40 000 km, à condition d'assurer des procédures de désulfatation périodiquement. Le critère de désulfatation (perte d'efficacité de 30%) est atteint au bout de 16 000 km. Il apparaît néanmoins clairement que la désulfatation n'est pas suffisante pour recouvrer le niveau initial de performances du système. Une conclusion importante de ce travail est que le nombre de désulfatations nécessaire dans le cas des cellules hexagonales est moindre que dans le cas des cellules carrées, du fait de l'épaisseur en moyenne plus faible du *wash-coat*.

Dans le cas du moteur de poids lourd, les travaux menés sur la base d'un monocylindre ont montré l'intérêt marqué de provoquer des périodes de régénération riches en CO (plutôt qu'en HC), ce qui a pour conséquence de déstocker les NO<sub>x</sub> plus rapidement et de les traiter plus efficacement. Avec un tel procédé, la pénalité en consommation pour atteindre un niveau de NO<sub>x</sub> < 3.5 g/kW·h est de 3%.

**Abstract — Application of NO<sub>x</sub> Adsorber to Diesel Depollution: performances and durability** — To ensure overall optimization of engine performance (NO<sub>x</sub>, particulates, efficiency), the use of a NO<sub>x</sub> after-treatment system appears necessary to meet the future Euro IV emissions standards and after. Among the known means, the NO<sub>x</sub> trap should offer an efficiency of the same order than the reduction by urea, without having the same constraints.

The trap operates on the basis of the alternation of operating phases with a lean mixture during which NO<sub>x</sub> is stored and rich phases during which nitrates are destored and treated. Important aspect of the technology, NO<sub>x</sub> adsorbers are very sensitive to sulfur poisoning and future fuel standards are unlikely to be sufficient to prevent the system from requiring periodic desulfation procedures.

The present paper presents results obtained on a light duty application, on a one hand, on a heavy duty case on a second hand.

In the light duty front, the purpose of the work presented first, was to study the effects of low fuel sulfur content such as 50 ppm and 10 ppm on the NO<sub>x</sub> adsorber efficiency for a Diesel application. Through this study, the influence of the substrate cell geometry has also been assessed.

The use of a 10 ppm sulfur fuel is not enough to maintain, at a high level, the NO<sub>x</sub> adsorber performance during a 40 000 km aging test. The desulfation criterion (efficiency loss of 30%) is reached after the first 16 000 km. However, the desulfation operation is not enough to recover the initial catalyst performance and the poisoning velocity increases as the catalyst ages.

The hexagonal cell substrate catalyst is less sensitive to sulfur poisoning than a square cell substrate catalyst so that its desulfation frequency is much lower. With a 10 ppm sulfur fuel, 4 desulfation operations were achieved with a hexagonal cell catalyst as opposed to 11 with a square cell catalyst during the 40 000 km aging test.

In the heavy duty application, the investigation, using a single-cylinder engine, demonstrated that the best NO<sub>x</sub> emission/fuel consumption trade-off are obtained with destorage richer than stoichiometry. These destorage conditions could be obtained in various configurations (injection timing, EGR, post-injection). The various adjustments tested show the advantage of producing a large amount of carbon monoxide to obtain fast destorage and efficient treatment of the trapped nitrates. With a method like this, the extra fuel consumption resulting from the succession of rich/lean phases is around 3% for an emission objective of NO<sub>x</sub> < 3.5 g/kW-h. By mounting a second trap in parallel, an oxidation catalyst, or using EGR, this result can be significantly improved.

The gradual storage of sulfur contained in fuel limits the trapping capacity of the NO<sub>x</sub> system, necessitating periodic desulfation. Various configurations have been tested to purge the sulfates. Mass spectrometer exhaust gas analysis makes it possible to quantify COS, H<sub>2</sub>S and SO<sub>2</sub> emissions during this phase. Nevertheless, the tests have shown the limits of the possibilities in a single cylinder installation.

## NOTATIONS

AFR	Air/fuel ratio
°CA	Crank angle degree
CO	Carbon monoxide
CO <sub>2</sub>	Carbon dioxide
COS	Carbonyl sulfide
dBA	Decibel (noise unit)
DeNO <sub>x</sub>	After-treatment technic aimed at abatting NO <sub>x</sub> in lean burn engines
DW10ATED	PSA 2 l, direct injection, common rail, turbocharger, engine
ECU	Engine control unit
EGR	Exhaust-gas recirculation
EVC	Exhaust-valve closing
EVO	Exhaust-valve opening
GSV	Gas space velocity

HC	Hydrocarbons
H <sub>2</sub> S	Hydrogen sulfide
I VO	Intake valve opening
NO <sub>x</sub>	Nitrogen oxydes (NO, NO <sub>2</sub> )
NO	Nitrogen monoxide
NO <sub>2</sub>	Nitrogen dioxide
rpm	Round per minute
ppm	Part per million
ppmC	Part per million carbon
SO <sub>2</sub>	Sulfur dioxide
SO <sub>3</sub>	Sulfur trioxide.

## INTRODUCTION

Diesel engines offer a significant advantage in terms of fuel consumption and, therefore, in terms of CO<sub>2</sub> emissions.

However, this technology remains confronted with the issue of particulate matter and nitrogen oxides. New diesel engines, equipped with common-rail injection systems and advanced engine management control, allow drastic decreases in the production of these pollutants. Nevertheless, the contribution of exhaust-gas after-treatment in the ultra low emission vehicles conception has become unavoidable today.

The elimination of  $\text{NO}_x$  produced by lean burn engines has been the subject of numerous developments [1-5].  $\text{NO}_x$  adsorber technology is an efficient solution to the  $\text{NO}_x$  issue over quite a wide temperature range. Its working principle is as follows: in lean conditions, NO is oxidized on a precious metal site such as platinum by oxygen to  $\text{NO}_2$ . Next, this  $\text{NO}_2$  migrates on the catalytic surface towards the adsorption sites such as alkali metal or alkaline earth trapping materials to create a nitrate. To recover the  $\text{NO}_x$  storage capacity, periodic switches from lean to rich mixture are required so as to reduce the stored  $\text{NO}_x$  to  $\text{N}_2$  with reductants such as hydrogen, carbon monoxide and hydrocarbons. However, this technology remains confronted with the issue of sulfur poisoning whatever the  $\text{NO}_x$  trap catalyst formulation may be [6]. The mechanism for sulfur poisoning is assumed to be similar to the mechanism for  $\text{NO}_x$  trapping [7].  $\text{SO}_2$  produced by lean burn engines is oxidized to  $\text{SO}_3$  by the platinum and reacts with wash-coat compounds forming a sulfate on the trapping material. Unfortunately, the sulfates formed are more stable than the nitrate species and cannot be desorbed during the periodic rich pulses if the exhaust-gas temperature remains lower than  $550^\circ\text{C}$ , leading to a loss of the  $\text{NO}_x$  storage capacity [8]. If high exhaust gas temperature and low air/fuel ratio lead to the desulfation of the  $\text{NO}_x$  adsorber [9], the catalyst support cell structure can also make the desulfation process easier [10].

The present paper contains two main parts:

- The first one deals with  $\text{NO}_x$  adsorber applied to light duty engine.
- The second one deals with  $\text{NO}_x$  adsorber applied to heavy duty engine.

## 1 LIGHT DUTY APPLICATION

### 1.1 Experimental Set Up

This study has been achieved with a DW10ATED engine that equips the *Peugeot* 406 HDI vehicle. It is a direct injection Diesel engine with a common-rail injection system, two valves per cylinder, a cooled EGR circuit, an intake throttle and a turbocharger with inter cooler (see Fig. 1). Its main characteristics are as follows:

- bore: 85 mm;
- stroke: 88 mm;
- displacement:  $1.997\text{ cm}^3$ ;
- compression ratio: 18:1;
- maximum power: 80 kW at 4000 rpm;
- maximum torque: 260 Nm at 1750 rpm.

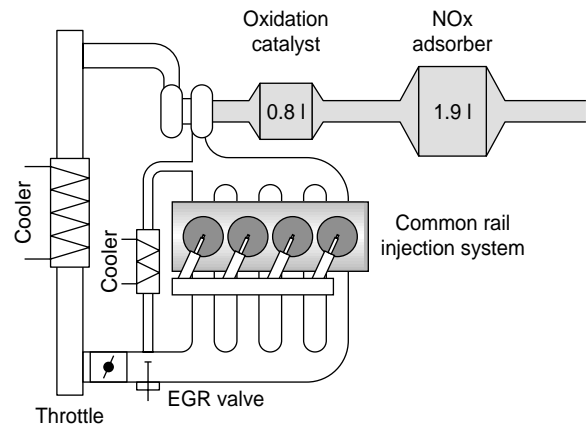


Figure 1

Engine set up – Peugeot 21 HDI.

Two catalysts were introduced on the exhaust line. The first one was an oxidation catalyst located just at the outlet of the turbine:

- monolith volume : 0.8 l;
- monolith material : ceramic;
- cells per square inch/thickness (mil): 400/6.5;
- precious metal: platinum;
- precious metal load:  $50\text{ g/ft}^3$  (1 ft = 30.48 cm), soit  $1.76\text{ kg/m}^3$ .

The second catalyst, located 90 cm downstream from the Light Off catalyst, was a  $\text{NO}_x$  adsorber:

- monolith volume: 1.9 l;
- monolith material: ceramic;
- cells per square inch/thickness (mil): 400/6;
- precious metal load:  $210\text{ g/ft}^3$  (1 ft = 30.48 cm), soit  $7.40\text{ kg/m}^3$ ;
- platinum/palladium/rhodium: 10/10/1.

Concerning the  $\text{NO}_x$  storage component, it is only possible to mention that it is alkali metals and/or alkaline-earth based  $\text{NO}_x$  storage component, the formulation and preparation method are proprietary to the supplier.

Two types of cell geometry were used for the  $\text{NO}_x$  adsorber, the classic square cell and the less common hexagonal cell. The same wash-coat quantity was laid down on the two types of catalyst. The wash-coat is better distributed on a hexagonal cell catalyst limiting, in particular, the washcoat thickness in the corner areas. Ikeda *et al.* [11] have shown that a thin wash-coat presents advantages with regard to catalyst activity and poisoning. Indeed, in a first step,  $\text{NO}_x$  adsorption takes place on washcoat surface sites, then, as the trap is being loaded,  $\text{NO}_x$  affect sites in depth.  $\text{NO}_x$  release and reduction are more efficient and faster with surface sites, unlike  $\text{NO}_x$  on deeper sites because of reactant

diffusion velocity. Thus, the catalytic surface in direct contact with exhaust gas needs to be increased. Moreover, thickness reduction may be useful to limit sulfur poisoning since sulfur poisoning mechanisms are likely to be very close to the  $\text{NO}_x$  trapping one.

The fuel used for this study is a diesel fuel, stemmed from a hydrocracking refining process. Its basic characteristics are as follows:

- cetane number: 58;
- %C: 86%;
- %H: 13.7%;
- density (15 °C): 829.4 kg/m<sup>3</sup>;
- sulfur content: 5 ppm;
- distillation curve:  $T_{5\%} = 220^\circ\text{C}$                        $T_{95\%} = 352^\circ\text{C}$

To prevent the injection system from failing, a sulfur free lubricant additive has been blended to the fuel.

The engine lubricant oil was a commercial *Esso* 15W40 with a sulfur content of 0.43%.

For the aging procedure, the fuel sulfur content has been adjusted with a sulfured additive.

The  $\text{NO}_x$  emissions at the  $\text{NO}_x$  adsorber inlet and outlet were followed simultaneously by two chemi-luminescence based analyzers (Cosma Topaze 3000 and Pierburg CLD PM 2000). The sulfur emissions were measured, in line, with a VF mass spectrometer.

*IFP* has developed a specific engine management system that represents an essential element of the experimental set up with regard to the  $\text{NO}_x$  adsorber management. Indeed, to be efficient, the  $\text{NO}_x$  adsorber requires periodic switches between lean and rich conditions. A change in the injection and air parameters has to be applied to the engine so as to meet the right conditions for regenerating the  $\text{NO}_x$  adsorber. Of course, this change has to have no impact on the driveability. To achieve this, two sets of cartography have been established, one for the lean mode and another for the rich mode. The bench computer triggers the switch between the two sets of engine maps (*Fig. 2*).

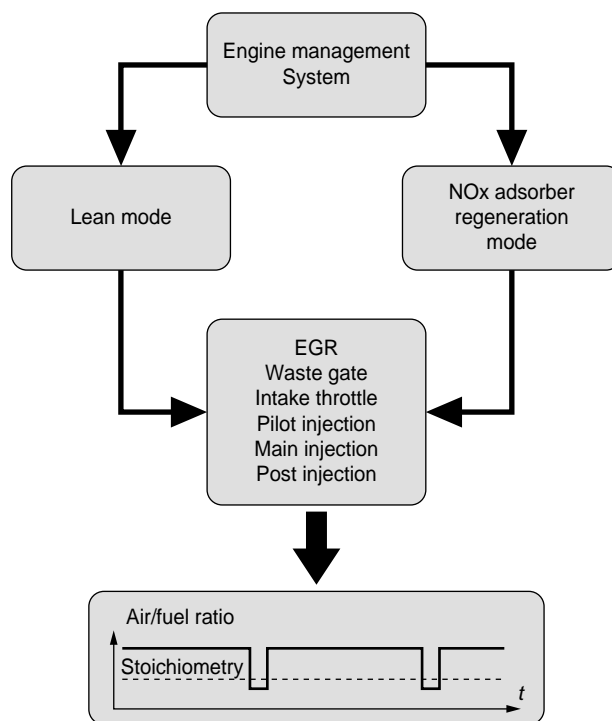


Figure 2

AFR modulation for  $\text{NO}_x$  adsorber regeneration.

## 1.2 Aging Cycle

The  $\text{NO}_x$  adsorbers have been aged, at the engine test bench, with the repetition of specific cycles that are described in Table 1.

The first aging cycle would correspond to a mean vehicle speed of 50 km.h<sup>-1</sup> (with a *Peugeot* 406 HDI vehicle) and is mainly focused on urban driving conditions with a mean exhaust-gas temperature of 260°C (*Fig. 3*). The second one

TABLE 1  
Aging cycles

	Cycle no. 1 ("cold" cycle)	Cycle no. 2 ("hot" cycle)
35" (1250 rpm – 24 N·m) 51" (1250 rpm – 48 N·m) 5" (idle)	× 10	× 10
145" (2150 rpm – 76 N·m) 30" (3000 rpm – 140 N·m) 30" (2150 rpm – 76 N·m) 20" (idle)	× 1	× 20
Cycle duration	18 min 55 s	90 min 10 s
Mean calculated vehicle speed	50 km·h <sup>-1</sup>	87 km·h <sup>-1</sup>
Cycle fuel consumption	2.2 kg·h <sup>-1</sup>	4.35 kg·h <sup>-1</sup>

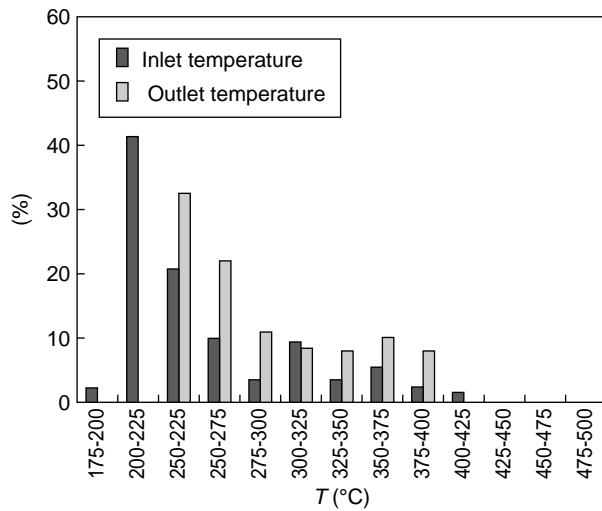


Figure 3  
NO<sub>x</sub> adsorber temperature breakdown according to temperature range on the aging cycle no. 1.

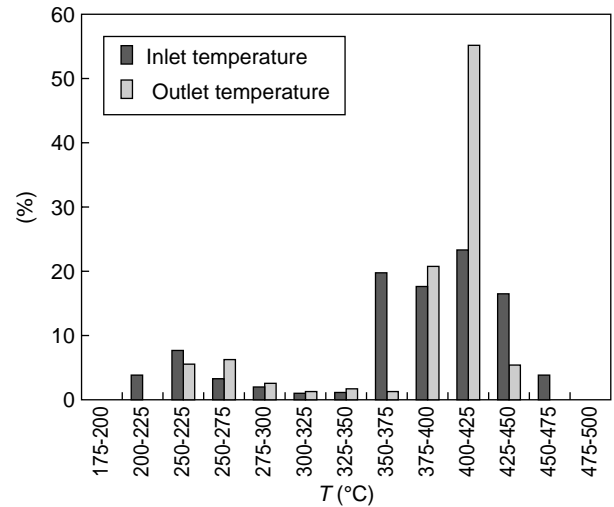


Figure 4  
NO<sub>x</sub> adsorber temperature breakdown according to temperature range on the aging cycle no. 2.

TABLE 2

NO<sub>x</sub> adsorber regeneration calibration

		1250 rpm - 48 N·m		2150 rpm - 76 N·m	
		Lean	Rich	Lean	Rich
AFR		30.2	13.7	26.4	13.8
Fuel quantity	kg/h	1.6	2.85	4.3	8.1
MAP	mbar	1060	995	1250	1120
CO*	(%)	0	2.9	0	2.1
HC*	ppmC	60	8000	50	800
O <sub>2</sub> *	(%)	11	1.5	9.2	1
Smoke	B.U	0.5	3	1.1	4

\* No<sub>x</sub> adsorber inlet.

would correspond to a mean vehicle speed of 87 km·h<sup>-1</sup> and to extra urban driving conditions with a mean exhaust-gas temperature of 375°C (Fig. 4). Whatever the aging cycle, the NO<sub>x</sub> adsorber regeneration is triggered, approximately, every 60 s on the two following engine conditions: 1250 rpm – 48 N·m and 2150 rpm – 76 N·m. The NO<sub>x</sub> adsorber regeneration mode lasts 12 s for the first engine condition and 10 s for the other. These NO<sub>x</sub> regeneration procedures were quite long so as to prevent the NO<sub>x</sub> adsorber from being partially regenerated.

The different characteristics of the regeneration points are given in Table 2. The aim of these calibrations was to obtain an air/fuel ratio lower than 14.5, with the highest carbon monoxide level, which is the best component for NO<sub>x</sub> desorption and reduction, and with the lowest oxygen and hydrocarbon level. To do so, a change in both mass air flow and injected fuel quantity was achieved. The mass air flow was decreased with a full opening of the waste gate, with the

intake throttle closing and by maintaining a small opening of the EGR valve, the position of which is limited by the smoke emissions. By decreasing drastically the mass air flow, a first increase of the fuel quantity is necessary to keep the torque constant. However, it is generally not enough to reach the right AFR. Therefore, the engine output is still decreased by delaying the pilot and the main injections, which leads to another increase of the injected fuel quantity to maintain the torque. Finally, a post injection is added which has a beneficial effect on the smoke emissions but which may lead to oil dilution issues.

The oxidation catalyst located upstream from the NO<sub>x</sub> adsorber also has a beneficial effect on the NO<sub>x</sub> adsorber efficiency. First, it decreases the emission of unburned hydrocarbons produced by the engine (which also increases the CO content and decreases the O<sub>2</sub> content). Second, through exothermic reactions, it helps to reach higher level of temperature when a desulfation procedure becomes necessary.

The NO<sub>x</sub> adsorber efficiency was calculated by integrating the mass NO<sub>x</sub> emission at the inlet and outlet of the catalyst:

$$\text{Efficiency} = 100 * \left( 1 - \frac{\int_0^{1010} \text{NO}_x \text{ - downstream} \cdot dt}{\int_0^{1010} \text{NO}_x \text{ - upstream} \cdot dt} \right)$$

This integration was done under the same conditions whatever the aging cycle (see Fig. 5). When the NO<sub>x</sub> adsorber efficiency ranged from 60% to 65%, a SO<sub>x</sub> regeneration procedure was triggered. This procedure consisted of keeping the AFR equal to 13.18 and the exhaust-gas temperature, at the inlet of the NO<sub>x</sub> adsorber, equal to 680°C for 12 min. This was determined by following the evolution of the sulfur emissions at the outlet of the NO<sub>x</sub> adsorber with a mass spectrometer until these emissions reached zero. This is a lengthy process incompatible with a real application. In a real application, NO<sub>x</sub> adsorber poisoning rates had to be much lower so as to reduce the length of the desulfation procedure.

The oil dilution rate was followed during the aging procedure (see Fig. 6). It was useful to check the quality of the regeneration mode calibrations. Indeed, the use of the post injection may drastically increase the oil dilution and may lead to huge lubrication issues and engine damage. The oil dilution rate was also used to calculate accurately the engine oil consumption in order to obtain the oil contribution in the sulfur emission. So, with a 10 ppm sulfur fuel, the oil

contribution to the sulfur emission in the exhaust gas is equal to 11.6% and is equal to 2.6% with a 50 ppm sulfur fuel (on the aging cycle no. 1).

### 1.3 NO<sub>x</sub> Adsorber Poisoning with the “Cold” Cycle

A first evaluation of the NO<sub>x</sub> adsorber poisoning has been achieved with the cold aging cycle, the characteristics of which are given above. The tests were done with two fuel sulfur contents, 50 ppm and 10 ppm, and with two types of catalyst cell geometry: square and hexagonal (see Table 3).

TABLE 3

Aging test conditions

Abbreviation	Cell geometry	S-content	Duration	Mileage
H_10	Hexagonal	10 ppm	800 h	40 000 km
C_10	Square	10 ppm	800 h	40 000 km
H_50	Hexagonal	50 ppm	200 h	10 000 km
C_50	Square	50 ppm	200 h	10 000 km

#### 1.3.1 Efficiency Loss

As mentioned before, sulfur is known to be a strong poison for NO<sub>x</sub> adsorbers. Even the use of a 10 ppm sulfur fuel is not enough to prevent the catalyst from being poisoned. As shown on Figure 7, the small amount of SO<sub>2</sub> produced by the engine is enough to poison the catalyst and to induce a loss of efficiency. Indeed, the desulfation criteria are reached

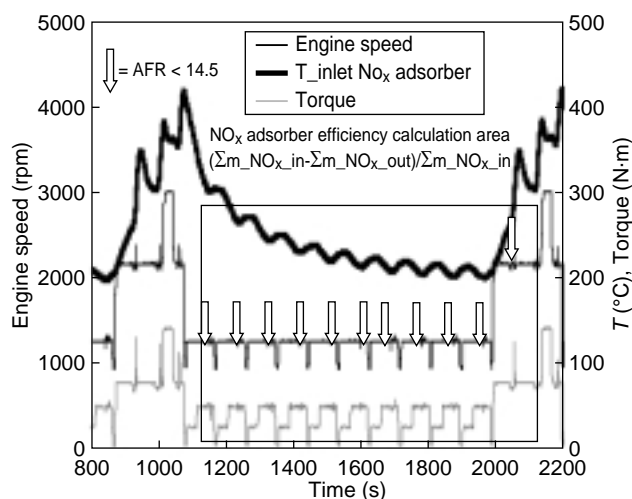


Figure 5

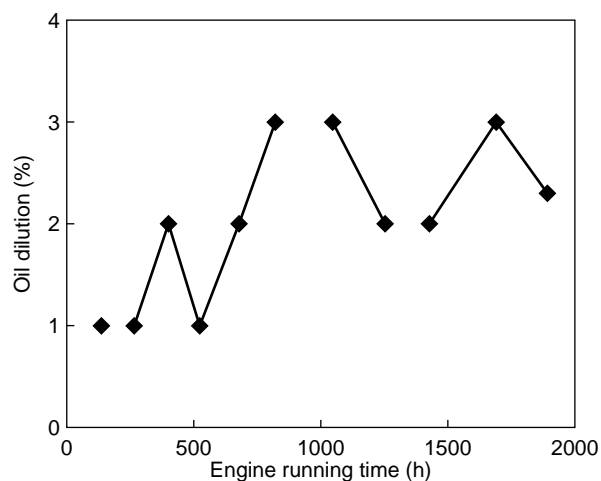
NO<sub>x</sub> adsorber efficiency calculation.

Figure 6

Oil dilution versus engine running time.

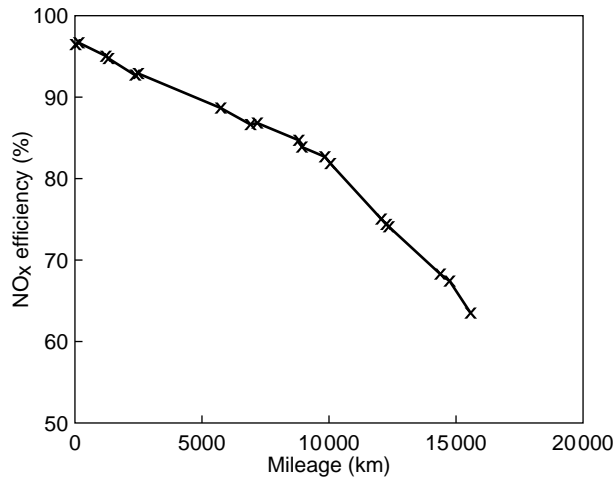


Figure 7  
NO<sub>x</sub> efficiency decrease – Aging cycle no. 1 – 10 ppm sulfur fuel – Hexagonal cell.

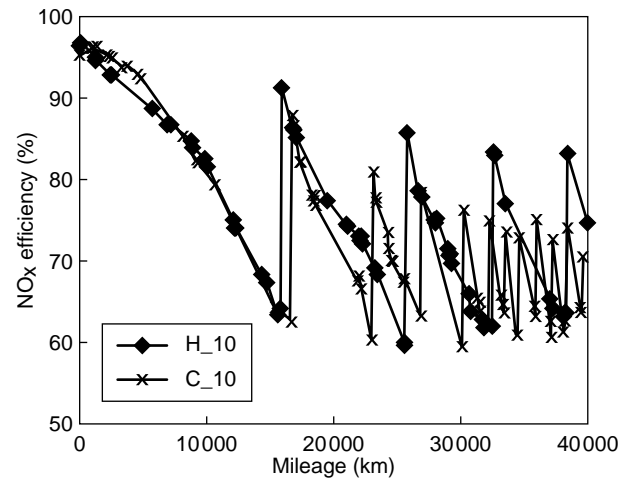


Figure 8  
Influence of cell geometry on sulfur poisoning – Aging cycle no. 1 – 10 ppm sulfur fuel.

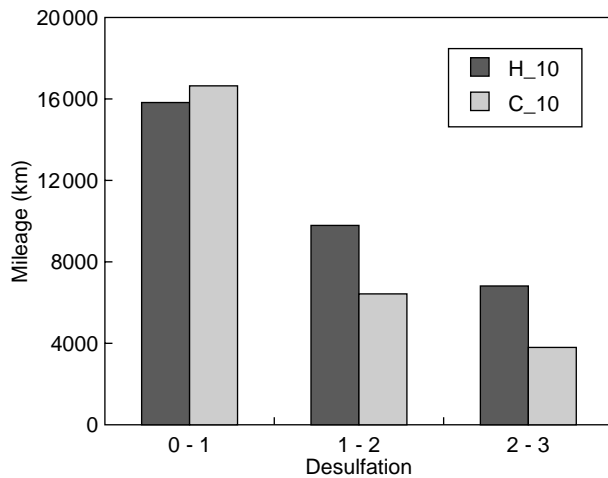


Figure 9  
Mileage evolution between two desulfation procedures – Aging cycle no. 1 – 10 ppm sulfur fuel.

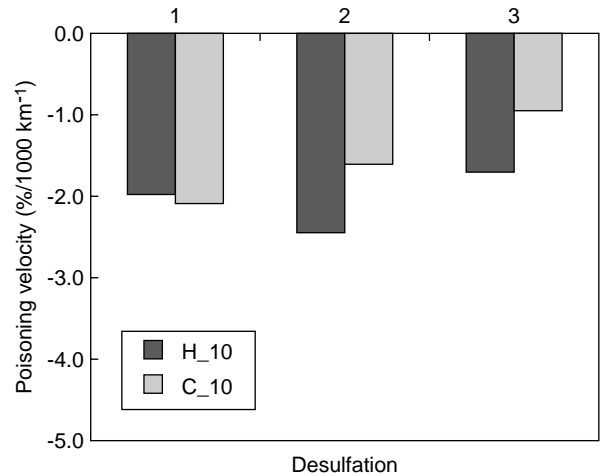


Figure 10  
Cell geometry influence on poisoning velocity – Aging cycle no. 1 – 10 ppm sulfur fuel.

after 16 000 km. Thus, even with a low fuel sulfur content, a desulfation procedure is unavoidable to keep the NO<sub>x</sub> adsorber performance at a high level.

### 1.3.2 Geometry Impact

To assess the influence of the channel geometry, two catalysts, one with hexagonal cells, the other with square cells, have been aged over 40 000 km with a 10 ppm sulfur fuel. The NO<sub>x</sub> efficiency evolution is plotted versus mileage on Figure 8.

Until the first 16 000 km and the first desulfation procedure, no difference can be noticed between the two types of catalyst. However, as the aging procedure goes further, the square cell catalyst activity decreases much more quickly leading to a higher desulfation frequency so as to maintain the NO<sub>x</sub> adsorber efficiency higher than 60%. If the fresh catalysts require a desulfation procedure after 16 000 km, the second and the third desulfation operation are only separated by 7000 km (hexagonal cells) and 4000 km



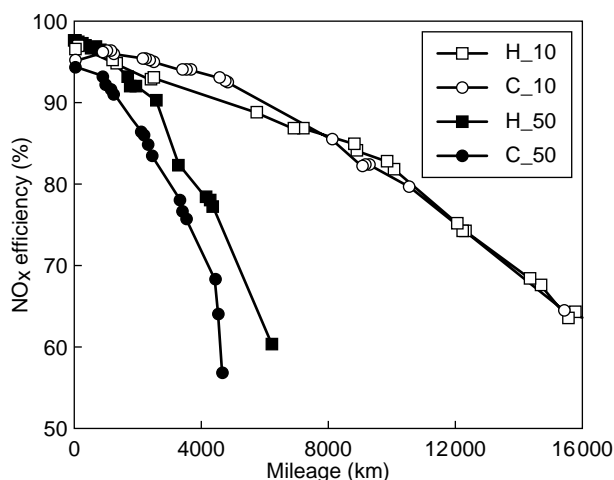


Figure 11

Fuel sulfur content influence on NO<sub>x</sub> conversion loss.

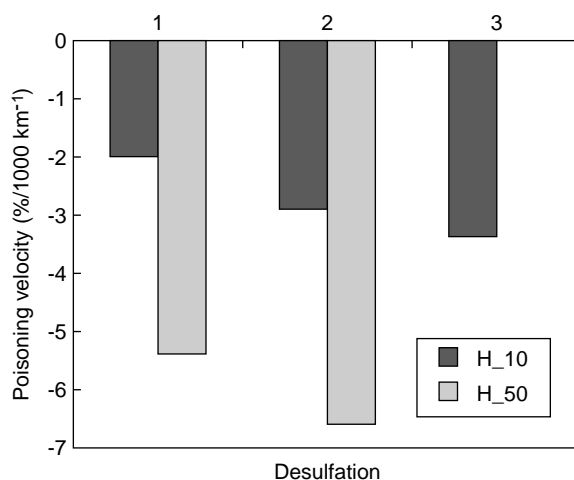


Figure 12

Influence of sulfur content on poisoning velocity.

(square cells) as shown on Figure 9. At the end of the test, a 40 000 km aged square cell catalyst requires a desulfation procedure every 1200 km.

To illustrate the efficiency loss, we have defined the poisoning velocity as the loss of efficiency per 1000 km. The mean poisoning velocity has been calculated between each desulfation procedure and a comparison between the two cell geometry is presented on Figure 10. This figure points out that the catalyst poisoning goes faster and faster and that the poisoning velocity is higher with a square section channel catalyst.

So, whatever the catalyst cell geometry, the poisoning velocity increases as the catalyst ages and the desulfation operation becomes less and less efficient with regard to the NO<sub>x</sub> storage capacity recovery. However, it appears that a hexagonal cell NO<sub>x</sub> adsorber is more sulfur resistant than a square cell catalyst.

### 1.3.3 Fuel Sulfur Content Impact

Figure 11 shows the deterioration of the NO<sub>x</sub> conversion efficiency versus mileage. Two fuel sulfur concentrations, 10 and 50 ppm, have been used.

Of course, the poisoning velocity depends on the fuel sulfur content. However, it is not proportional to this parameter. Indeed, for the same type of catalyst, the poisoning is only 2.5 faster with a 50 ppm sulfur fuel if compared to a 10 ppm sulfur fuel (*Fig. 12*). The sulfur emission due to engine oil consumption is not enough to explain this fact since the sulfur ratio, with oil contribution, is equal to 4.5.

As mentioned before, the desulfation operation does not allow the recover of the initial NO<sub>x</sub> efficiency. Part of the NO<sub>x</sub> storage capacity is irreversibly damaged (*Fig. 13*).

The use of an in line mass spectrometer has allowed us to follow the sulfur emissions during the desulfation operations. H<sub>2</sub>S is the main sulfur product emitted during the NO<sub>x</sub> adsorber desulfation. If the H<sub>2</sub>S emissions between the two types of catalyst are compared (*Fig. 14*), it appears that, for the same amount of sulfur produced by the engine, the sulfur release is weaker with a hexagonal cell catalyst.

All catalysts were analyzed by X-fluorescence technique in order to assess the amount of sulfur left in the catalyst after the last desulfation operation performed at the end of each aging test. Table 4 presents, for each configuration and for the whole endurance test, the sulfur mass emitted by the engine, the remaining sulfur mass on the catalysts (light off catalyst and NO<sub>x</sub> trap) and the associated NO<sub>x</sub> efficiency loss. A higher remaining sulfur mass is obtained when a hexagonal cell catalyst is used. This confirms that less sulfur releases occurred during the different desulfation operations (that were achieved with similar temperatures for all catalysts). However, it is quite surprising to observe that the most sulfur resistant catalyst is the one which presents the highest remaining sulfur mass. It means that there is not a direct relationship between the catalyst remaining sulfur mass and the catalyst efficiency loss.

TABLE 4

Sulfur balance

	40 000 km		10 000 km	
	H_10	C_10	H_50	C_50
Engine sulfur emissions	19.9 g	19.9 g	22.6 g	22.6 g
Remaining sulfur	2 g	0.75 g	1.65 g	1.15 g
Efficiency loss	14.8 g	27.1%	10.4%	10.6%

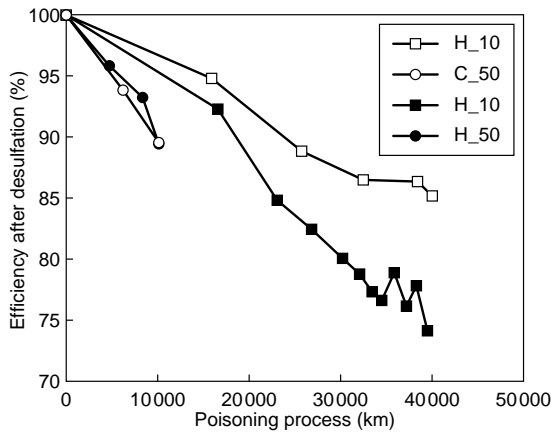


Figure 13  
Efficiency recovery after desulfation.

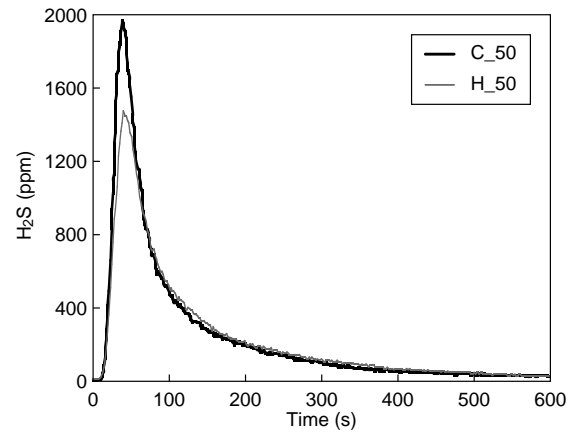


Figure 14  
H<sub>2</sub>S emission during desulfation procedure – Cumulative engine sulfur emission = 8 g.

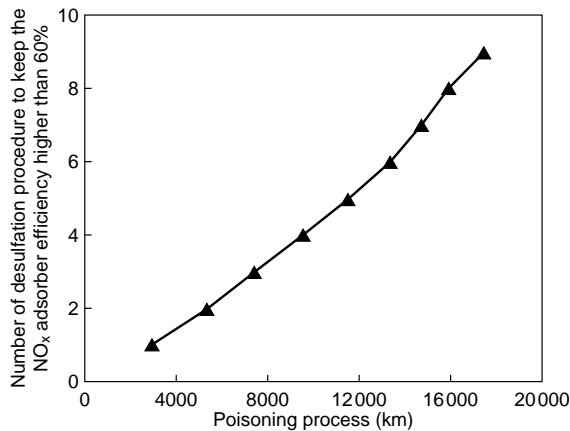


Figure 15  
Desulfation frequency – Aging cycle no. 2 – 50 ppm fuel sulfur content.

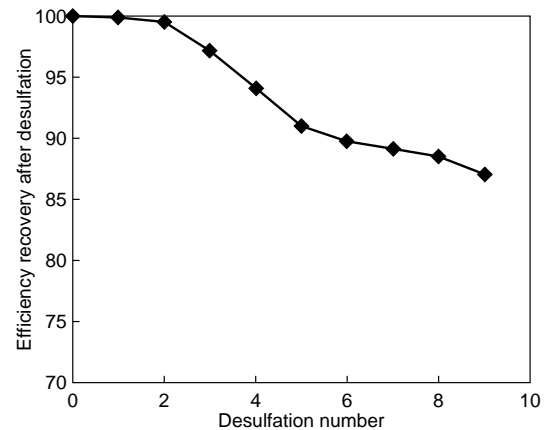


Figure 16  
Efficiency recovery after desulfation – Aging cycle no. 2 – Hexagonal cells – 50 ppm sulfur fuel.

### 1.4 NO<sub>x</sub> Adsorber Poisoning with the “Hot” Cycle

The evolution of the NO<sub>x</sub> adsorbers efficiency has also been followed with the aging cycle no. 2 (see Table 1). A hexagonal cell catalyst and a 50 ppm fuel sulfur content were used for this test. As for the aging cycle no. 1, a desulfation procedure is triggered so as to keep the NO<sub>x</sub> adsorber efficiency higher than 60%. The desulfation frequency is quite high, as shown on Figure 15. So, 9 desulfation procedures are necessary during the first 18000 km. The desulfation procedure fuel penalty, integrated on the 18000 km, is equal to 0.77%, which may appear reasonable. Nonetheless, the main difficulty of the NO<sub>x</sub>

adsorber desulfation, in a real application, is that a high level of temperature is required. Due to the thermal inertia of the exhaust line, the time you need to reach the right temperature may be quite long increasing the risk that a sudden break in the driving conditions occurs, leading to a stop of the desulfation procedure.

Figure 16 shows the evolution of recovery efficiency after the desulfation procedures. The first two desulfations appear to be very effective with total recovery of the initial NO<sub>x</sub> adsorber efficiency. However, as the aging goes further, the catalyst seems to be irreversibly damaged. So, after 18.000 km and 9 desulfation procedures, the NO<sub>x</sub> storage capacity is decreased by 23%.

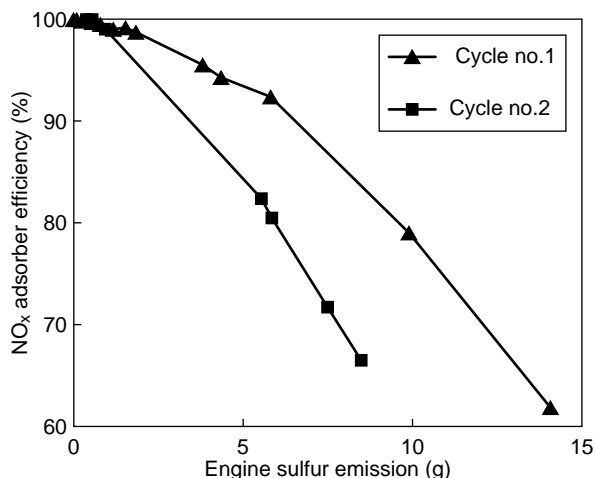


Figure 17

NO<sub>x</sub> adsorber efficiency *versus* engine sulfur emissions – Hexagonal cell catalyst – 50 ppm fuel sulfur content.

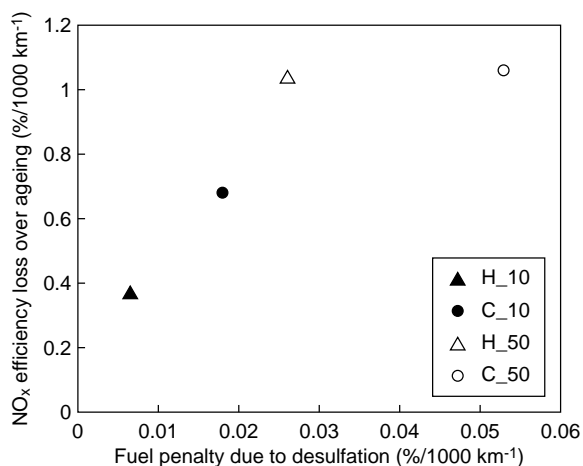


Figure 18

NO<sub>x</sub> efficiency loss *versus* desulfation fuel penalty – Aging cycle no. 1

A comparison between the two aging cycles (*see Fig. 17*) highlights that, for the same engine sulfur emission, the NO<sub>x</sub> adsorber deactivation is quicker with the aging cycle no. 2 than with the aging cycle no. 1. The main difference between the two cycles is the exhaust gas temperature level. It clearly appears that the temperature has a great impact on the NO<sub>x</sub> adsorber deactivation even if the exhaust gas temperature remains within a reasonable range (average of 260°C for the aging cycle n°1 and 375°C for the aging cycle no. 2).

### 1.5 NO<sub>x</sub> Adsorber System Viability

The influence of both catalyst geometry and fuel sulfur content has been highlighted above. Figure 18 allows a direct comparison between the different configurations. The NO<sub>x</sub> efficiency loss between the fresh catalyst and the desulfated aged catalyst is plotted *versus* the fuel penalty concerning the desulfation operations only. With a 50 ppm sulfur fuel, the hexagonal cell geometry clearly appears to lead to a lower fuel penalty when the efficiency loss is similar. With a 10 ppm sulfur fuel (and a longer aging), the use of as hexagonal cell catalyst leads to both a lower fuel penalty and a lower efficiency loss. Figure 18 also indicates that the decrease of the fuel sulfur content has a stronger beneficial effect than the catalyst cell geometry.

As demonstrated in previous papers [9, 12], the relationship between the NO<sub>x</sub> adsorber performance and the fuel sulfur content is not linear. If the distance required to get from the initial 95% NO<sub>x</sub> reduction to 65% NO<sub>x</sub> reduction is plotted *versus* the “equivalent” fuel sulfur content (equivalent meaning that the oil contribution is taken into account) the curve presents a power shape (*Fig. 19*). The interpolation curve equation would be:  $y = 221\,276 \times x^{-0.9271}$ .

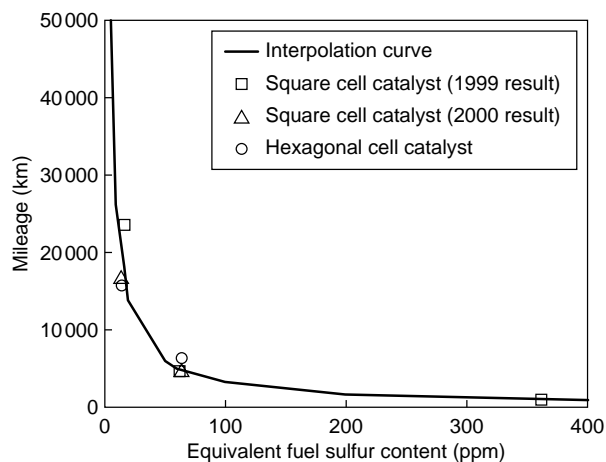


Figure 19

Influence of sulfur content on the mileage until the first desulfation operation.

This relationship lays a stress on the fact that NO<sub>x</sub> adsorbers are highly sensitive to sulfur content in fuel. So, a huge decrease in fuel sulfur content would lead not only to a better NO<sub>x</sub> adsorber durability but also to an easier management of the exhaust-gas after-treatment system. Indeed, to partly recover the NO<sub>x</sub> trap performance, a poisoned catalyst requires a desulfation operation, which means rich mixtures and high temperatures. These conditions are far from the usual Diesel engine conditions and quite hard to obtain. What is more, the thermal inertia of the exhaust line will strongly penalize the time required to meet the right desulfation conditions so that desulfation operations might conflict with other vehicle management constraints.

## 2 HEAVY DUTY APPLICATION

### 2.1 Experimental Set Up

#### 2.1.1 Engine - Installation

The test engine is a *Renault-VI* 120-45, single-cylinder direct injection supercharged research engine. Its main technical characteristics are indicated below:

- Description: MIDR 120-45
- Bore: 120 mm
- Stroke : 145 mm
- Displacement : 1640 cm<sup>3</sup>
- Compression ratio: 16:1
- Dead volume : 109.2 cm<sup>3</sup>
- Multi-cylinder head, 24 valves
- Swirl ratio: 1.25
- Supercharging: up to maximum cylinder pressure of 160 bar (1 bar = 0.1 MPa)
- Distribution : IVO = + 5°, EVC = + 5°  
EVO = + 43°, IVC = + 11°

Injection system:

- Injector holder Bosch Type C2
- Nozzle: DLLA 150 PV 31 87 12
- Bosch V33 ECU.

The injection system was controlled using a power box supplied by *IFP*. Thanks to its four power stages, it was possible to adjust independently up to four injected quantities and four timings. Therefore, it was possible to operate with injection modes such as: preinjection, main injection, post-injection and  $\text{DeNO}_x$  injection (injection when the exhaust valve is open). The injection pressure was still continue to be managed by the engine ECU.

#### 2.1.2 Exhaust Line

Because of the specific requirements of the single-cylinder engine exhaust line, and to obtain performance comparable to that of a multi-cylinder engine, several modifications have been made. The exhaust system was modified so as to incorporate a  $\text{NO}_x$  trap in the line. Because of the length and the very large volume of the single-cylinder engine exhaust line, modifications were required for test purposes. To obtain fast air/fuel ratio transition phases at the trap, we had to insert bypass valves in the system. The exhaust line equipped in this way was capable of circulating or not circulating exhaust gases through the trap. The temperature of the trap during the transition phases is get constant by a specific device.

#### 2.1.3 Fuels

In order not to perturb the efficiency of the trap during denitration tests, the fuel used is a sulfur-free hydrocracked Diesel fuel.

### 2.2 Denitration Tests

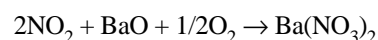
The purpose of this study is to evaluate the  $\text{NO}_x$  trap potential in terms of the fuel consumption/nitrogen oxide emission trade-off. The system works according to the following principle.

During the lean phase, nitrogen oxides are stored in a trap. To obtain this storage, the nitrogen oxides are oxidised by means of the platinum present in the monolith.

The reaction is as follows:

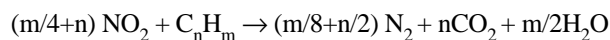
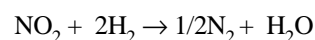
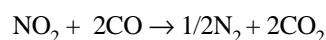


The nitrogen dioxide is then stored in the monolith by means of barium oxide in the form:



Operation at an equivalence ratio of more than 1 results in the destorage of the  $\text{NO}_2$  stored in the barium sites.

Reduction reaction:



is then obtained through the platinum and rhodium coating contained in the monolith.

#### 2.2.1 Use of Exhaust Gas Oxygen Sensor

The tests presented here are performed to determine accurately, by means of  $\lambda$  sensor, the end of the destorage phases. Successive tests with various destorage times duration make it possible to determine the optimum value.

If the destorage phase is too short, the trap is only partially regenerated. In this case, efficiency decreases much more quickly. If we analyze the  $\text{NO}_x$  emissions downstream of the trap, during storage phase, and compare the results with those obtained with an empty trap, we can determine the mass of  $\text{NO}_x$  that was not destored during the denitration phase.

A test was run by trapping, each time, the same mass of nitrogen oxides and using the same destorage point configuration; only the destorage duration was variable. Under these conditions, the following curve (*Fig. 20*) shows that a rich phase lasting more than 10 s is enough to obtain complete destorage.

For a shorter time, the trap is only partially regenerated. Destorage tests for times of less than 8 s were not performed.

The equivalence ratio measured by the lambda sensor is given in Figure 21.

First we observed that, initially, the downstream sensor has a “delay” when the equivalence ratio increases and as the exhaust gases begin to pass through the trap. The delay, lasting approximately 0.2 s as observed, corresponds to the time taken to fill the trap with engine exhaust gases.

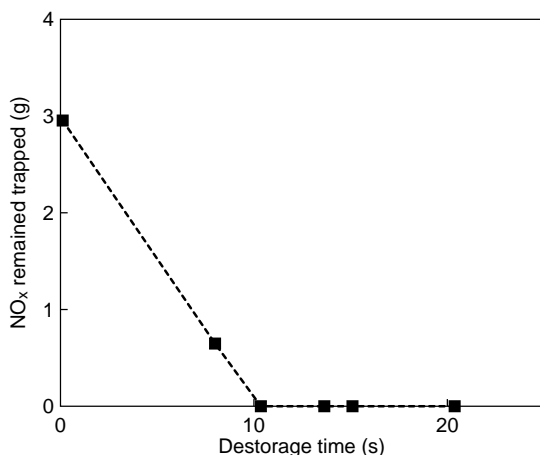


Figure 20  
Equivalence ratio effect.

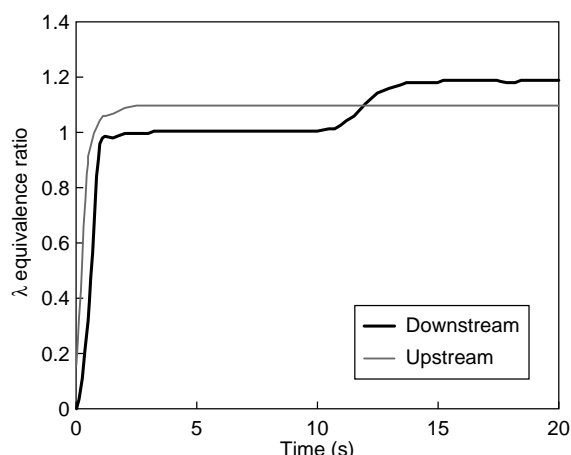
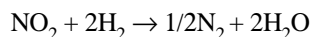
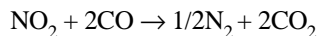


Figure 21  
Equivalence ratio λ signal.

Then, we observed that the equivalence ratio measured upstream of the trap is consistent with the gas composition analyzed at the engine outlet.

The equivalence ratio measured by the downstream sensor, on the other hand, is 1, due to the fact that the reactions:

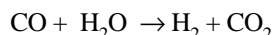


consume carbon monoxide and hydrogen contained in the exhaust gases.

In the case of operation at an equivalence ratio above 1, the oxygen concentration is almost 0. Under these conditions, without any CO, H<sub>2</sub> or O<sub>2</sub>, the downstream sensor indicates an equivalence ratio of 1.

When all the nitrates contained in the trap were destored and treated, the concentration of reducers downstream of the trap increases and the response of the downstream λ sensor exceeds 1. The time measured for the rising of the equivalence ratio sensor response is around 10 s. This time corresponds to the time observed during previous testing for complete nitrate destorage.

Then, the water gas shift reaction results in the reduction of carbon monoxide by water:



The response of the λ sensor to CO or H<sub>2</sub> differs considerably, explaining why the equivalence ratio measured downstream of the trap seems higher than that measured upstream.

The λ sensor signals therefore make it possible to determine accurately the time taken for total destorage of the nitrates trapped. Under these conditions, there is no longer any need to load the trap after destorage in order to check that it was entirely regenerated.

### 2.2.2 Stored NO<sub>x</sub> Quantity

Figure 22 shows NO<sub>x</sub> emissions upstream and downstream *versus* time.

We observed that the downstream emissions tend to increase slowly as the trap is progressively loaded with nitrates. After 280 s of storage, downstream emissions equal 90% of the NO<sub>x</sub> entering the trap. This is because continuous reduction of the NO<sub>x</sub> is obtained with in lean condition. The efficiency of this natural DeNO<sub>x</sub> is around 10%.

The quantity of nitrates stored as a function of time is indicated below. Note that efficiency decreases gradually as the sites still available diminish (*Fig. 23*).

Under these conditions, the maximum stored quantity is slightly greater than 5 g.

### 2.2.3 Stored Quantity Variation – Effect on Destorage

During this part of testing, the trap is always loaded in the same way. The destorage point correspond to an equivalence ratio of 1.09. The emissions of CO and HC are respectively 1140 and 85 g/h. We try to determine the time needed for total destorage of the NO<sub>x</sub>. The destorage strategy used will always be the same (*Fig. 24*).

The above curve shows the results obtained during these tests. Note that for stored quantities between 1 and 3 g, the destorage time is more or less constant. For larger quantities, the destorage of NO<sub>x</sub> is more difficult, thus explaining the increased destorage time.

When the quantity of NO<sub>x</sub> contained in the trap is small, the quantity of reducer is enough to reduce them gradually as they are desorbed. When a larger quantity is involved, nitrogen oxides are emitted downstream (*Fig. 25*).

For a quantity of 2.6 g contained in the trap, downstream emissions are low. When 5.2 g have been stored, downstream emissions are far higher.

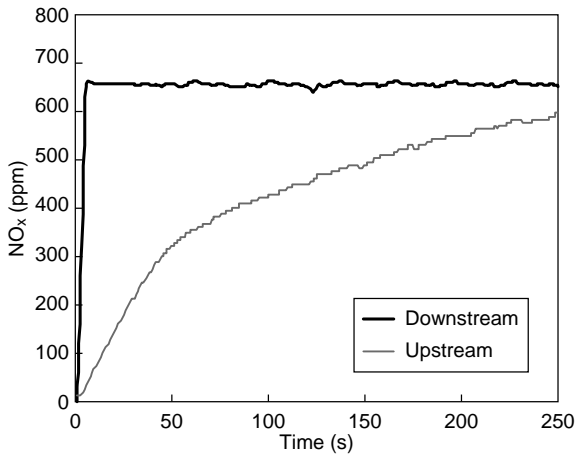


Figure 22  
Upstream/downstream  $\text{NO}_x$  emissions.

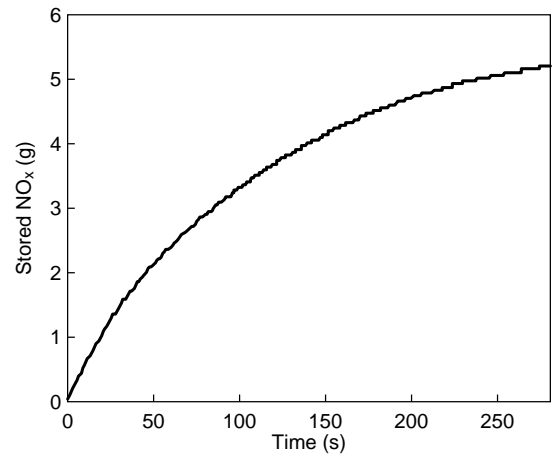


Figure 23  
Nitrates storage.

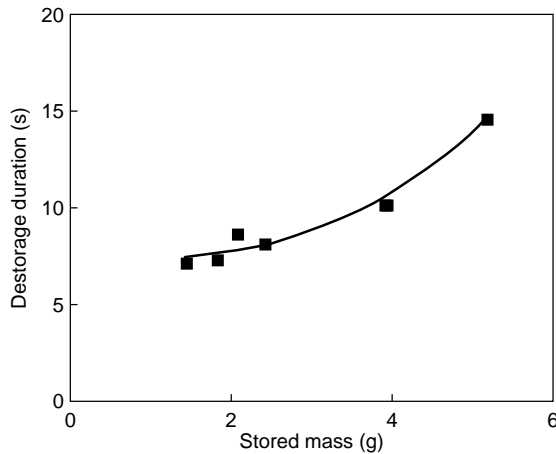


Figure 24  
Effect of stored quantity on destorage duration.

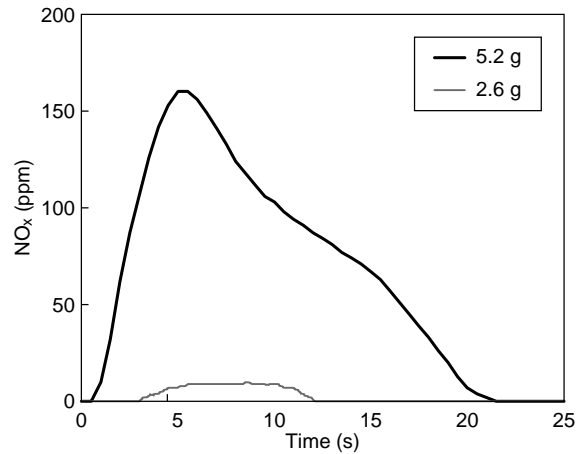


Figure 25  
 $\text{NO}_x$  destorage.

For a stored quantity of less than 2.5 g, there is no re-release. The rereleased fraction is 0.3% for a stored quantity of 3 g and reaches 1.3% for 5 g (Fig. 26).

These tests demonstrate the advantage of working with a stored mass less than 3 g. The destorage will not lead to a long rich operating phase. In addition, efficiency in terms of emitted  $\text{NO}_x$  storage will be high and  $\text{NO}_x$  slip will be limited.

For the chosen operating point, this will result in lean operation (the phase during which the  $\text{NO}_x$  is stored) lasting less than 90 s before the trap is regenerated.

#### 2.2.4 Influence of Destorage Equivalence Ratio

All these tests were performed with the same mass stored in the trap. The following curve (Fig. 27) shows the time needed

for complete destorage of nitrogen oxides contained in the trap as a function of rich phase equivalence ratio.

The gain in terms of denitration duration is high for equivalence ratios up to 1.15. Note that if a high equivalence ratio makes it possible to minimize fuel consumption, it does not offer the best performance in terms of overall nitrogen oxide emissions (lean + rich phases). This is due to the fact that we minimize the rich phase duration during which  $\text{NO}_x$  emission downstream of the trap is 0. Figure 28 shows the balance obtained with the overall storage/destorage phase.

#### 2.2.5 Influence of Destorage Engine Configuration

Subsequent to the destorage equivalence ratio variation tests, it has become clear that an equivalence ratio of 1.15 offers the best consumption/destorage time trade-off. Subsequent to

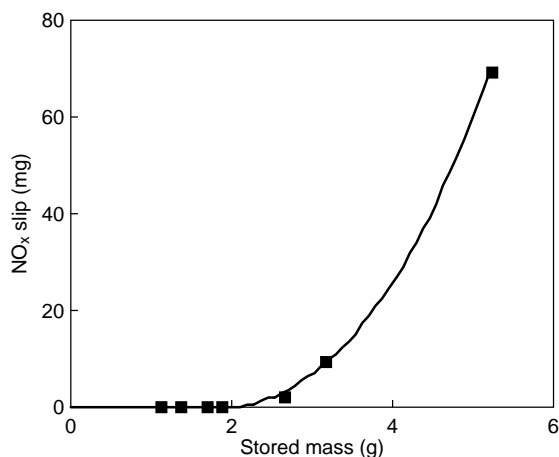


Figure 26  
Untreated NO<sub>x</sub>.

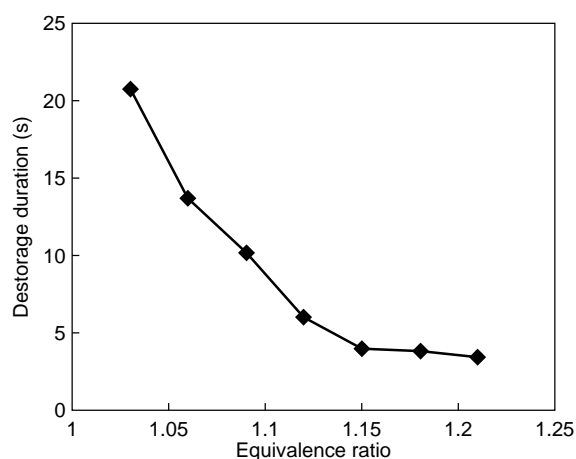


Figure 27  
Effect of equivalence ratio on NO<sub>x</sub> destorage duration.

the initial tests, there is little interest in testing at a higher mixture equivalence ratio. The second value was chosen arbitrarily at a value lower than 1.09.

For all these tests, 2 storage times of 30 and 60 s were chosen. Respectively, this allows the storage of a quantity of 1.1 g and 2 g.

All the tested configurations are shown in Table 5. They were tested for 2 loading ratios and 2 equivalence ratios (1.09 and 1.15). Points no. 5 and no. 6 were only tested for an equivalence ratio of 1.15.

TABLE 5  
Tested engine configuration

	Inject. timing (°CA)	Main inject. (%)	Pre-inject. (%)	Post-inject. (%)	Post-inj. timing (°CA)	EGR (%)
Pt. no. 1	6	100	–	–	–	–
Pt. no. 2	6	80	–	20	2	–
Pt. no. 3	6	80	–	20	100	–
Pt. no. 4	6	100	–	–	–	10
Pt. no. 5	6	90	10	–	–	–
Pt. no. 6	–2	100	–	–	–	–

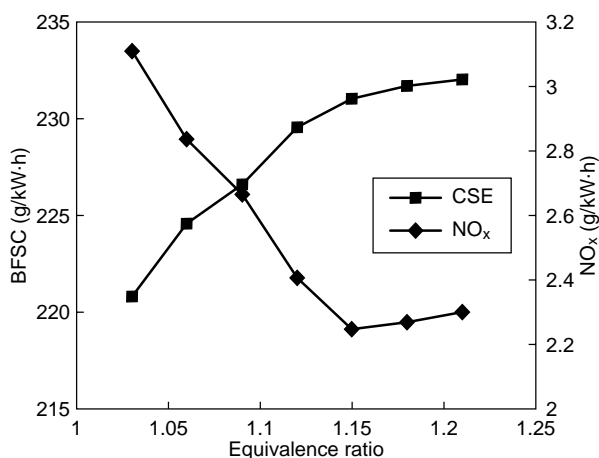


Figure 28  
Equivalence ratio effect on overall NO<sub>x</sub> emissions (lean + rich phases) and fuel consumption.

Compared to the standard injection configuration (Pt. no. 1), we observe the following consequences for the other configurations:

- The use of post-injection timed very close to main injection induces a smoke decrease. The emissions of CO and HC are almost equivalent to those of standard injection.
- Later post-injection is favorable to an increase in unburned hydrocarbons. The considerable degradation of efficiency means an increase in the GSV.
- The use of exhaust-gas recirculation leads to an increase in the residual oxygen in the exhaust gases. This negative effect is considerably reduced by operation at a very high equivalence ratio.
- Operation with preinjection is a way of considerably reducing the combustion noise, which drops from 89 to 85 dBA. The emission and GSV levels are unchanged.
- Retarded timing, by the lower efficiency, results in an increase of the GSV. The other parameters are generally

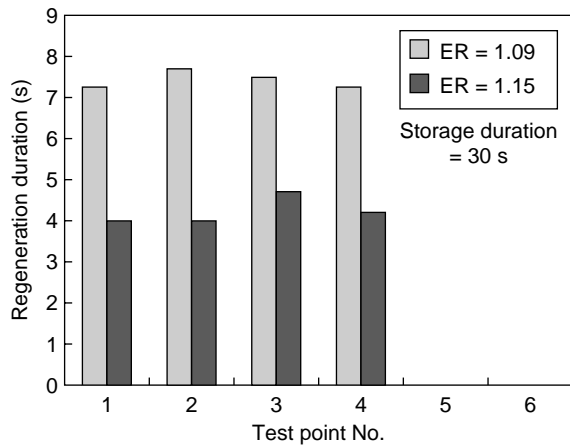


Figure 29

Storage quantity and engine configuration effect.

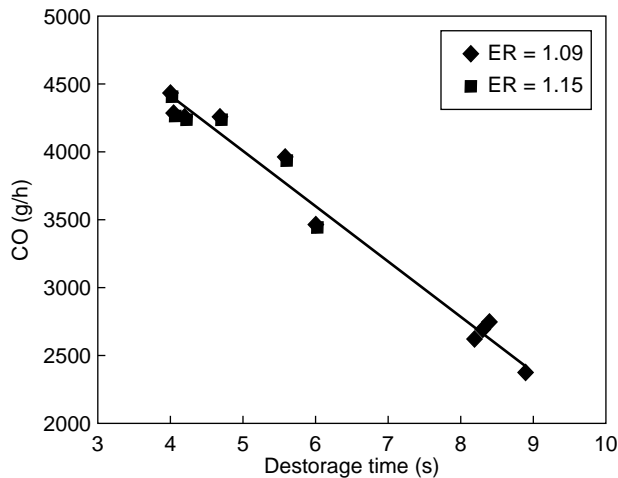
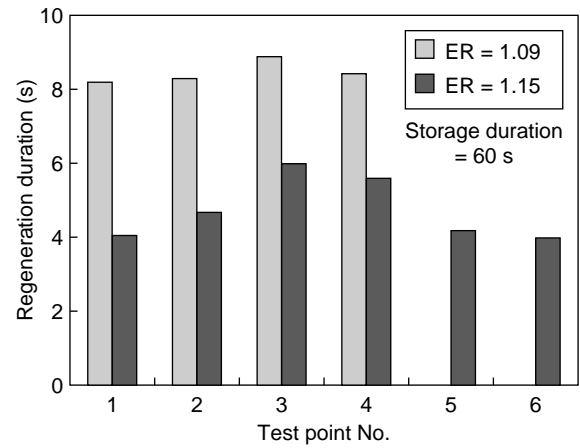


Figure 30

Influence of CO on destorage.

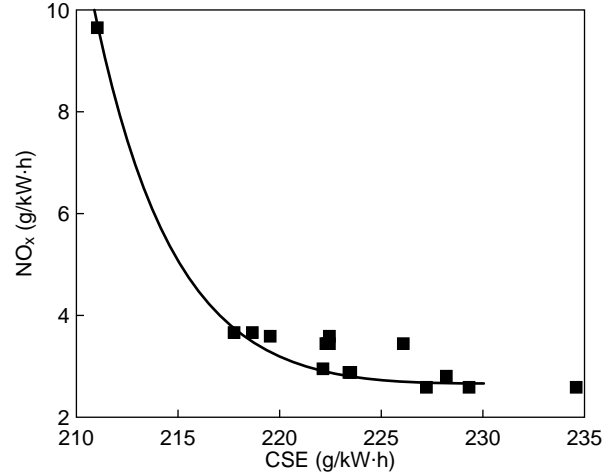


Figure 31

$\text{NO}_x$  emission/fuel consumption trade-off.

unchanged. Note that if the offset of combustion in the expansion stroke causes an increase in the exhaust temperature, the complexity of the line and its thermal inertia will not allow the difference to be perceived.

Note that, whatever configuration is used, a 1.15 equivalence ratio provides faster destorage.

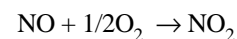
The main injection configuration alone then permits faster destorage (Fig. 29).

The analysis of the destorage time as a function of the previously investigated criteria (CO, HC,  $\text{O}_2$  and GSV) reveal considerable disparity of the results for the last three criteria mentioned.

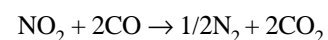
Note that CO is the first order parameter for destorage. Indeed, as shown in the following curve, the time taken to

destore the nitrogen oxides contained in the trap is proportional to the flow of carbon monoxide in the engine (Fig. 30).

All these points correspond to a  $\text{NO}$  stored mass of 2 g. First, they are oxidised by means of the platinum. The reaction is as follows:



This corresponds to a mass of 3.07 g of trapped  $\text{NO}_2$ . The reduction reaction is as follows:



The mass of CO needed for the oxidation of nitrogen dioxide contained in the trap is therefore 3.73 g. It is thus evident that the efficiency of the reaction varies according to



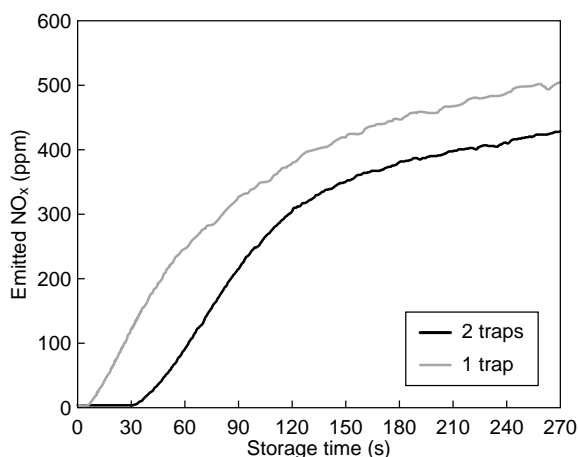


Figure 32  
Trap volume effect.

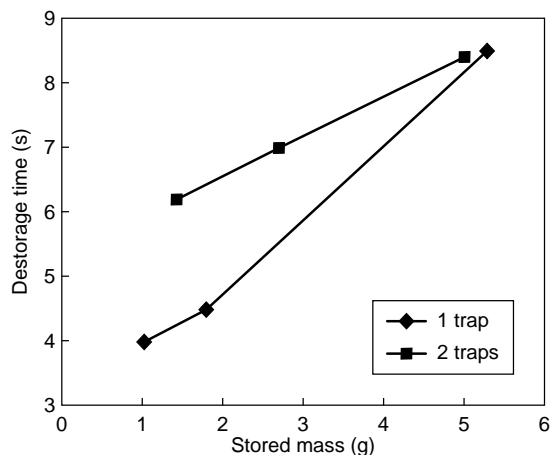


Figure 33  
Trap volume effect on destorage duration.

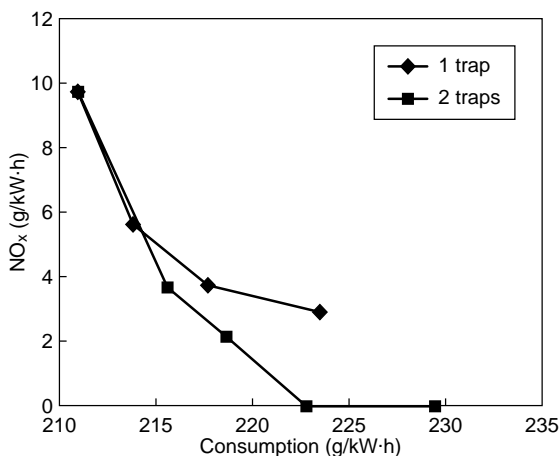


Figure 34  
 $\text{NO}_x$  emission/fuel consumption trade-off improvement.

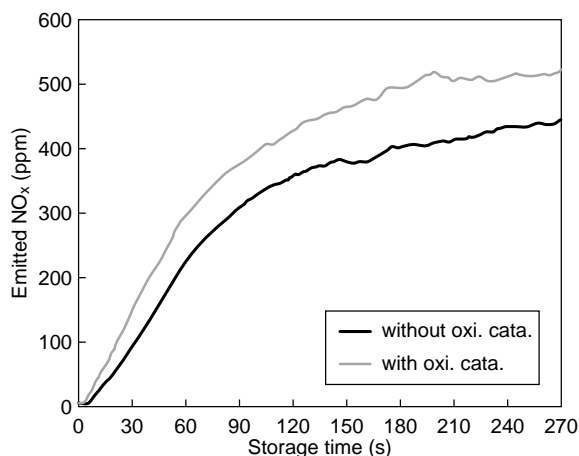


Figure 35  
Oxidation catalyst effect.

the injection configuration. Note that even in the most favorable case, destorage efficiency is only 76%. In the least favorable case, it is 58%. Nevertheless, it is evident that the most efficient configurations are obtained with operation at an equivalence ratio of 1.15.

All of the tested points fit in with the  $\text{NO}_x$  emission/fuel consumption trade-off. Overall, the best positioned points are those obtained with destorage at equivalence ratio 1.15 (Fig. 31).

Under these conditions, it will be seen that the extra consumption generated by an imposed  $\text{NO}_x$  level of 3.5 g/kW.h would be around 3.5%. This corresponds to operation including a storage phase of 60 s and destorage lasting 4 s.

## 2.2.6 Effect of Trap Volume

Tests have been conducted by setting up 2 traps in parallel to establish the efficiency of an increased trap capacity in terms of a  $\text{NO}_x$  emission/fuel consumption trade-off.

Figure 32 shows  $\text{NO}_x$  emissions at the outlet of this setup, gradually as the trap fills.

The trap storage capacity is increased. It changes from 5 g to more than 7 g for 270 s storage. The destorage time is also higher in the case of 2 traps connected in parallel, as shown in the following curve (Fig. 33).

Although the destorage time is longer for the same mass of stored  $\text{NO}_x$ , the emission/consumption balance is still positive (Fig. 34). This is due to the increased efficiency in nitrogen oxide storage.

In particular, note that it is possible to store all the emitted NO<sub>x</sub> and operate with zero nitrogen oxide emission providing that storage time is less than 30 s.

### 2.2.7 Influence of Oxidation Catalyst

The results obtained during desulfation tests led us to complete the denitration tests by testing a setup with an oxidation catalyst upstream of the NO<sub>x</sub> trap. It is clear that the trap storage capacity for a duration of 270 s increases from 5 to more than 6.5 g in the oxidation catalyst case (Fig. 35). Table 6 shows the results obtained in terms of balance between NO/NO<sub>x</sub>.

In the case of operation without an oxidation catalyst, the following values (Table 6) are obtained:

TABLE 6  
NO<sub>x</sub> emissions without oxidation catalyst

	Engine outlet	Trap outlet
NO (ppm)	620	500
NO <sub>x</sub> (ppm)	640	520

The values obtained at the outlet of the trap correspond to those obtained when the trap is saturated. In this configuration, nitrogen oxide emissions at the engine outlet comprise approximately 95% NO. The balance remains the same at the outlet of the trap. For this setup, the natural DeNO<sub>x</sub> of the trap is around 18%.

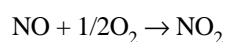
The measurements made with the oxidation catalyst gave the following values (Table 7):

TABLE 7  
NO<sub>x</sub> content with oxidation catalyst

	Engine outlet	Ox. cat. outlet	Trap outlet
NO (ppm)	615	330	330
NO <sub>x</sub> (ppm)	640	640	450

This operating point corresponds more or less to that studied previously. In this case, the nitrogen oxides content is approximately 95% NO.

At the oxidation catalyst outlet, the NO content is 50% lower due to the reaction:



The result is a natural DeNO<sub>x</sub> that reaches 30%. Indeed, natural DeNO<sub>x</sub> seems more efficient with NO<sub>2</sub> than with NO. Assembling this oxidation catalyst is therefore a way of obtaining gain of around 0.5% on fuel consumption for the same NO<sub>x</sub> emission target.

## 2.3 Desulfation Test

### 2.3.1 Installation Modification

An oxidation catalyst was mounted upstream of the NO<sub>x</sub> trap to obtain a higher gas temperature. This temperature increase will be obtained by oxidizing the unburned hydrocarbons and the carbon monoxide with the residual oxygen contained in the exhaust gases. The purpose of this operation was to obtain a trap inlet temperature of at least 650°C and therefore efficient desulfation of the trap.

Subsequent to the various problems encountered, due the considerable length of the exhaust line, the adjustment of the equivalence ratio and temperature will be made by injecting air into the exhaust gases downstream of the exhaust gas damping capacity. Under these conditions, it was possible to obtain 2 operating equivalence ratios (1.5 and 1.10) at 2 temperatures (650°C and 750°C).

Table 8 gives an example of an operating point at an equivalence ratio of 1.10 and a temperature of 650°C at the inlet of the NO<sub>x</sub> trap.

TABLE 8  
Engine configuration

Equ. ratio		1.252	1.105
HC	ppmC	2 295	2 453
CO	%	7.988	6.662
CO <sub>2</sub>	%	9.70	8.54
O <sub>2</sub>	%	0.26	2.66
NO <sub>x</sub>	ppm	294	231

The first column of Table 8 corresponds to the values measured at the engine outlet, and the second, to those obtained after dilution by 10 kg/h of air. Under these conditions, oxidation of HC and CO in the catalyst produces an increase in the gas temperature from 350 to 650°C.

### 2.3.2 Procedure

The purpose of the tests is to assess the various trap desulfation procedures. Indeed, during operation with fuel containing sulfur, it will be gradually stored in the trap, causing an NO<sub>x</sub> efficiency loss.

### 2.3.3 Sulfating Cycle

To obtain the gradual poisoning of the trap by sulfur, a nitration/denitration cycle was established. It consists of a succession of phases: lean/rich. Considering the specific aspects of the single cylinder, it was not possible to obtain step form equivalence ratio transitions. The equivalence ratio profile is as follows (Fig. 36).

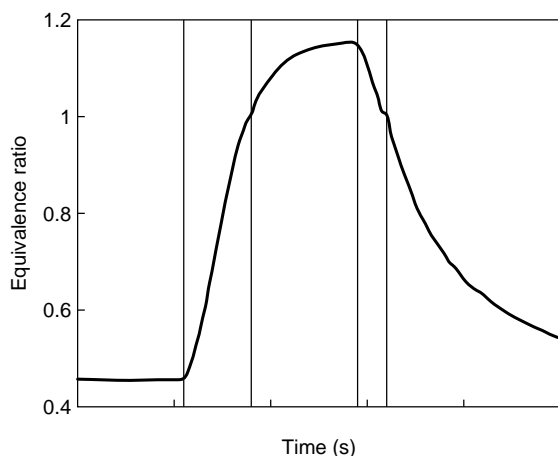


Figure 36  
Equivalence ratio transition.

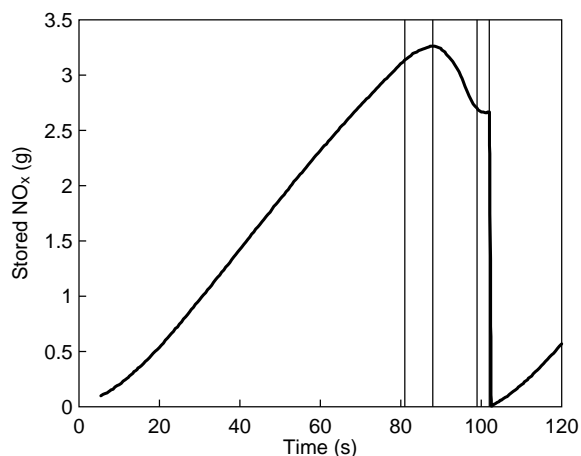


Figure 37  
NO<sub>x</sub> storage evolution.

Figure 37 shows the evolution of the NO<sub>x</sub> storage during this cycle.

It is clear that during the lean phase, 3.25 g of nitrogen oxides were trapped. Changing to an equivalence ratio above than 1 results in the releasing of 0.6 g, corresponding to 18% of the stored mass. It is clear that this high downstream emission is due to a smooth transition of the equivalence ratio. The previous tests resulted in the release of 15 mg for the same mass of stored nitrogen oxides.

Cycle validation was carried out using sulfur-free fuel to obtain constant efficiency as a function of time.

#### 2.3.4 Tests with 500 ppm Fuel

Fuel consumption during the tests was 6 kg/h. This corresponds to a mass of sulfur of 6 g passing through the trap for 2 h operation. It leads to the gradual poisoning of the trap.

This is characterized by increasingly large emissions of NO<sub>x</sub> downstream of the trap (Fig. 38).

The maximum value of NO<sub>x</sub> emitted just before the increase in the equivalence ratio was 175 ppm at the beginning of the test. It increases to more than 330 ppm after 2 h of operation. Under these conditions, the relative efficiency of the trap drops by 15% (Fig. 39).

During the tests, and because it was impossible to measure accurately the sulfur at the trap outlet, it is difficult to estimate accurately the quantity of sulfur stored in the trap.

#### 2.3.5 Desulfation

Destorage at an equivalence ratio of 1.10 was tested. The engine was set up as explained in the procedure. The species analyzed by a mass spectrometer are SO<sub>2</sub>, H<sub>2</sub>S and COS.

Details of the results of analysis are given in Figure 40. Most of the stored sulfates are released after a dead time of around 35 s in the form of H<sub>2</sub>S for 90% of the mass and COS for the remainder. After 8 min of operation, it is evident that no further sulfur destorage is taking place. The total extracted mass is around 1 g.

Under these conditions, the relative efficiency of NO<sub>x</sub> storage obtained after desulfation is 93%, probably due to a nontotal desulfation. If only half of the lost NO<sub>x</sub> storage efficiency was recovered, it's probably because only half of the active storage sites have been desulfated. As the desulfation phase only made it possible to extract 1 g of sulfur, the quantity of sulfur stored was therefore probably only 2 g. This corresponds to approximately 1/3 of the quantity contained in the burned fuel.

Following a further poisoning procedure, another desulfation test was carried out at an equivalence ratio of 1.05. Under these conditions, the sulfur contained in the trap was destored after approximately 30 s of operation and, unlike the previous test at equivalence ratio 1.10, was released in the form of SO<sub>2</sub>. After 20 s more, H<sub>2</sub>S and COS were emitted. The greater part of the sulfur that could be extracted from the trap was released after 250 s of operation, corresponding to a mass of 1 g as during the previous test (Fig. 41).

In the same way as for the previous tests, the trap recovers approximately 90% of its initial efficiency. A desulfation test after 1 h of storage (instead of 2 h) was also carried out. Sulfur emissions during destorage are comparable to those obtained previously (in terms of distribution). But the total destored mass is only 0.6 g for 1 g of sulfur that was stored. This tends to demonstrate that during sulfating, the sulfur stored first is the most difficult to extract.

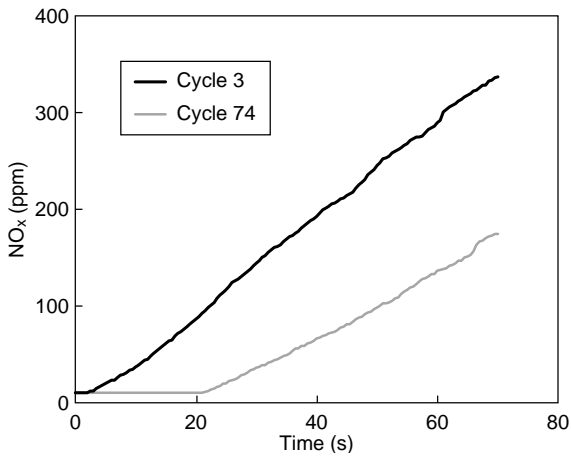


Figure 38  
Outlet  $\text{NO}_x$  emissions.

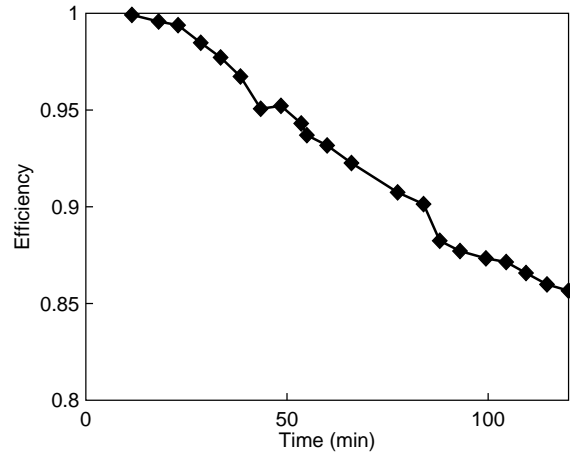


Figure 39  
Trap poisoning.

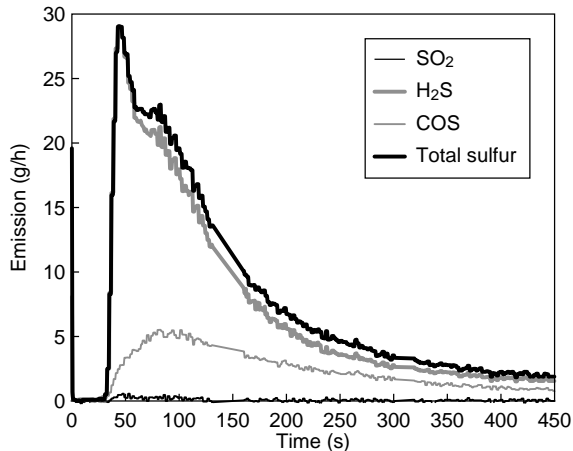


Figure 40  
Outlet sulfur emissions at equivalence ratio: 1.10.

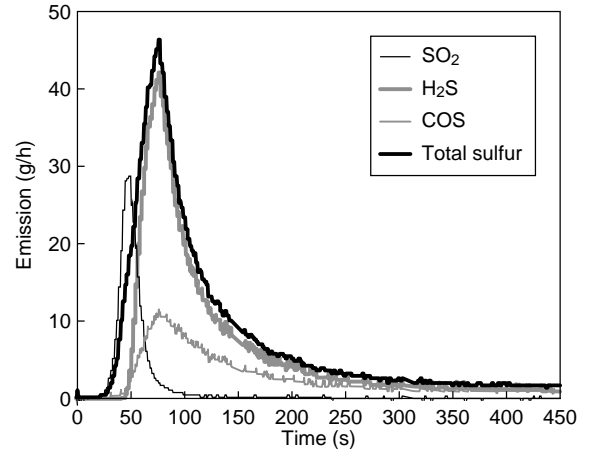


Figure 41  
Outlet sulfur emissions at equivalence ratio: 1.05.

### 2.3.6 Tests with 50 ppm Fuel

The purpose of the tests performed with a high sulfur fuel was to obtain accelerated poisoning of the trap. Operation with a less sulfur fuel leads to slower trap poisoning and a slower loss of efficiency. The following curve shows the efficiency losses compared between the 2 different fuels (Fig. 42).

If we express the loss of efficiency with respect to the mass of sulfur that passed through the trap, it becomes clear that the poisoning of the trap is comparable whatever fuel is used (Fig. 43). In this case, operation with a high sulfur fuel leads to faster poisoning, but comparable to operation with fuel containing little sulfur.

The distribution between the various emitted pollutants ( $\text{H}_2\text{S}$ ,  $\text{COS}$ ,  $\text{SO}_2$ ) is comparable to that obtained for desulfuration at  $R = 1.10$  during tests with the 500 ppm fuel (Fig. 40).

## CONCLUSIONS

The main conclusions reached at the end of this work are the following.

### Light Duty Application

An engine test bench procedure has been developed so as to assess Diesel  $\text{NO}_x$  trap performance in urban or extra-urban

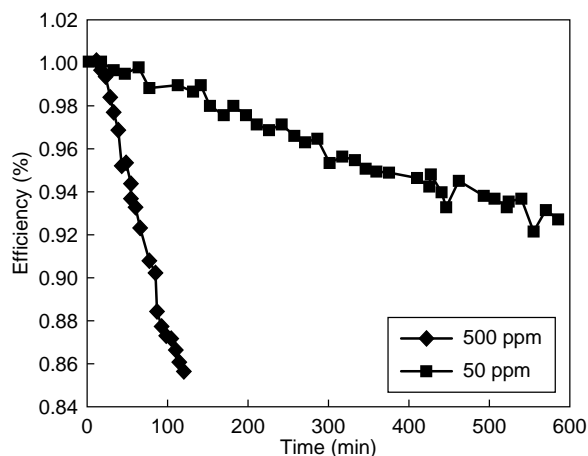


Figure 42

Trap efficiency loss (vs time).

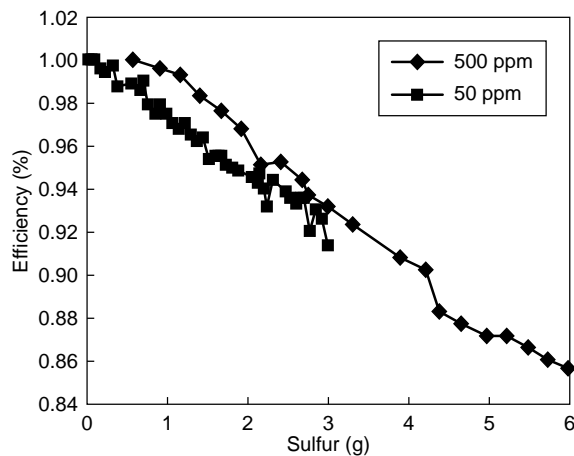


Figure 43

Trap efficiency loss (vs sulfur quantity).

driving conditions. The use of an advanced engine management system was necessary to make the diesel engine running in rich conditions for both  $\text{NO}_x$  and  $\text{SO}_x$  regeneration.

$\text{NO}_x$  adsorbers appear to be very sulfur sensitive and the use of a 10 ppm sulfur fuel is not enough to prevent the catalyst from being poisoned and requiring desulfation operations. This represents a real challenge for Diesel engines, the running conditions of which are far from the desulfation criteria and especially the desulfation temperature.

As the catalyst ages, the poisoning velocity goes faster and faster. The desulfation procedures allow the sulfur desorption to occur as  $\text{H}_2\text{S}$ . However they do not lead to total recovery of the initial catalyst efficiency.

The  $\text{NO}_x$  adsorber deactivation is, of course, a function of the fuel sulfur content. The relationship between  $\text{NO}_x$  adsorber poisoning rate and fuel sulfur content appears to have a nonlinear shape.

The  $\text{NO}_x$  adsorber poisoning appears to be temperature dependent. Indeed, the poisoning velocity is higher with a  $375^\circ\text{C}$  average exhaust gas temperature than with  $260^\circ\text{C}$ .

The use of a hexagonal cell catalyst instead of a square cell catalyst limits the  $\text{NO}_x$  adsorber deactivation. Four desulfation operations are required during a 40 000 km aging test to keep the  $\text{NO}_x$  adsorber efficiency higher than 60% as opposed to 11 with a square cell catalyst.

### Heavy Duty Application

This study gave us the opportunity to make an initial evaluation of the potential of a  $\text{NO}_x$  trap for the depollution of a heavy duty vehicle Diesel engine.

Initially, the study revealed extensive engine configuration possibilities for changing to an equivalence ratio above 1. Various injection and intake configurations were tested. In all cases, operation was stable and the thermal stress appeared below that acceptable by the engine.

The storage/destorage tests on the nitrates made it possible to optimize the trap denitration configuration. Essentially, tests were carried out at operating point mid load/mid speed. The comparison of the equivalence ratio  $\lambda$  sensor signals mounted upstream and downstream of the trap gave us the exact duration of the trap denitration phase. The initial tests enabled us to determine an optimum destorage equivalence ratio in terms of the trade-off between destorage time/consumption/ $\text{NO}_x$  emissions for the overall rich/lean operation. In a standard injection configuration, the equivalence ratio of 1.15 gives the best result. Various engine configurations for destorage (injection timing, post-injection, EGR, etc.) were also tested for various mass of nitrates stored in the trap. In all cases, the best results were obtained with the standard operating configuration, *i.e.* without EGR and with main injection only. All the tested configurations revealed that the main parameter for obtaining the fast denitration of the trap is large production of CO.

Assembling 2 traps in parallel made it possible to gain far more efficient storage of  $\text{NO}_x$  during the lean phase. Because the destorage time is not much different from a single trap operation, the  $\text{NO}_x$  emission/fuel consumption compromise is improved.

Assembling an oxidation catalyst upstream of the trap oxidizes most of the NO emitted by the engine. This facilitates the storage of nitrogen oxide. This setup therefore improves the efficiency of the trap, giving a more favorable emission/consumption trade-off.

The results obtained in terms of over-consumption for an objective of 3.5 g/kW·h of NO<sub>x</sub> compared to the standard point (10 g/kW.h) varies between 2 and 3.5% depending on the chosen configuration.

Trap sulfur poisoning tests have demonstrated the limits of the single-cylinder engine possibilities for the optimization of desulfation phases (during these tests, the exhaust temperatures were not sufficiently stable due to the line configuration). Nevertheless, it was possible to obtain usable results for this phase. The first tests performed with a 500 ppmS fuel indicated fast deterioration of the trap capacities. Under these conditions, the loss of efficiency was around 15% after 2 h of operation. Following desulfation, at an equivalence ratio of 1.05 or 1.10, we recover half the efficiency lost. The quantity of sulfur that is rereleased is around 1 g for a quantity of 6 g passing through the trap. Accordingly, it can be assumed that approximately 1/3 of the sulfur contained in the fuel was stored in the trap. Most of the sulfur contained in the trap is released in the form of H<sub>2</sub>S. The sulfur containing species emitted during this phase also depends on the destorage equivalence ratio. However, a major fluctuation in the trap inlet gas temperature revealed the limits of testing possibilities on a single-cylinder engine. The tests also revealed the need for operation with a low sulfur content fuel so as not to deteriorate too quickly the storage capacity of the trap nitrates.

As compared to SCR catalysis, NO<sub>x</sub> trap technology could appear as a potential challenger in the future, but still needs to be optimized in terms of fuel consumption and sulfur tolerance.

## ACKNOWLEDGEMENTS

The authors acknowledge the *Groupement scientifique moteurs (GSM with Renault SA, PSA Peugeot Citroën and IFP)*, the FSH (Fond de soutien aux hydrocarbures) for having supported this work.

## REFERENCES

- 1 Naoto, M., Shin'ichi, M., Kenji, K., Toshiaki, T. and Harada, Jun. (1995), Development of New Concept Three-way Catalyst for automotive Lean Burn Engines. *SAE 950809*, Detroit, 1995.

- 2 Bögner, W., Kraemer, M., Krutzsch, B., Pischinger, S., Voigtlaender, D., Wenninger, G., Wirbeleit, F., Brogan, M.S. and Brisley, R.J. (1995) Removal of Nitrogen Oxides from the Exhaust of a Lean Tune Gasoline Engine. *Applied Catalysis B – Environmental* 7.
- 3 Lütkemeyer, G., Weinowski, R., Lepperhoff, G., Wilkins, A.T.T., Brogan, M.S. and Brisley, R.J. (1996) Comparison of De-NO<sub>x</sub> and Adsorber Catalysis to Reduce NO<sub>x</sub> Emissions of Lean Burn Gasoline Engines. *SAE 962046*, San Antonio Texas, USA, 1996.
- 4 Brogan, M.S., Brisley, R.J., Moore, J.S. and Clark A.D. (1996) Evaluation of NO<sub>x</sub> Adsorber Catalyst System to Reduce Emissions of Lean Running Gasoline Engines. *SAE 962045*, San Antonio, Texas, USA, 1996.
- 5 Fekete, N., Kemmler, R., Voigtländer, D., Krutsch, B., Zimmer, E., Wenninger, G., Strehlau, W., van den Tillaart, J. A.A., Leyer, J., Lox, E.S. and Müller, W. (1997) Evaluation of NO<sub>x</sub> Storage Catalysts for Lean Burn Gasoline Fueled Passenger Cars. *SAE 970746*, Warrendale Pennsylvania USA, 1997.
- 6 Hodjati, H., Semelle F., Bert, C., Mouaddib-Moral, N. and Rigaud, M. (2000) Impact of Sulfur on NO<sub>x</sub> Trap Catalyst Activity – Poisoning and Regeneration Behavior. *SAE 2000-01-1874*, Paris, France, 2000.
- 7 Hepburn, J. S., Thanasiu, E., Dobson, D.A. and Watkins W. L. (1996) Experimental and Modeling Investigations of NO<sub>x</sub> Trap performance., *SAE 962051*, San Antonio, Texas, USA, 1996.
- 8 Dou, D. and Bailey, O.H. (1998) Investigation of NO<sub>x</sub> Adsorber Catalyst Deactivation. *SAE 982594*, San Francisco, California, USA, 1998.
- 9 le Faou, Ph., Guyon, M. and Bert, C. (1998) Impact of Sulfur on NO<sub>x</sub> Trap Catalyst Activity – Study of the Regeneration Conditions. *SAE 982607*, San Francisco, California, USA, 1998
- 10 Matsumoto, S., Ikeda, Y., Suzuki, H., Ogai, M. and Miyoshi, N. (2000) NO<sub>x</sub> Storage-Reduction Catalyst for Automotive Exhaust with Improved Tolerance Against Sulfur Poisoning . *Applied Catalysis B: Environmental* 25.
- 11 Ikeda, I., Sobue, K., Tsuji, S. and Matsumoto, S. (1999) Development of NO<sub>x</sub> Storage-Reduction Three-way Catalyst for D-4 Engines. *SAE 1999-01-1279*, Detroit, USA, 1999.
- 12 Guyon, M. and Blanche, P. (2000) NO<sub>x</sub> Trap System Developments and Characterization for Diesel Engines Emission Control. *SAE 2000-01-2910*, Baltimore, USA, 2000.

*Final manuscript received in November 2002*